**Supplemental Information**

**Supplemental Materials and Methods**

## Plasmid Constructs

The following DNA constructs were previously published and used in this study: Mito-DsRed and GFP-Tubulin (Clontech, Mountain View, CA); RFP-Sec61β (Shibata et al, 2008); eYFP-STIM1 wild type and eYFP-STIM1 10A (Smyth et al, 2012); DIC2C-RFP (Blasier et al, 2014); pEGFPC2-p150 (Moughamian & Holzbaur, 2012); HA-Aurora A K162R and HA-Aurora A T288D (Kashatus et al., 2011); Tom20-mCherry-FKBP (Miyamoto et al, 2012); HA-KIF5B MD-FRB, HA-BICD2-FRB, PEX-RFP-FKBP (Kapitein et al, 2010); GFP-Mito and GFP-BICD2-Mito (Hoogenraad et al, 2003); KHC-eCFP (Cai et al, 2007); myc-hMilton1 and HA-Miro1 (Pekkurnaz et al, 2014). Milton 28A was synthesized (GenScript, Piscataway, NJ) with the 28 alanine mutations (Figure S4A) in a pCMV tag 3A vector in order to match with the wild type construct used in our studies (Pekkurnaz et al, 2014).

## Immunoreagents

For immunofluorescence of HeLa, COS7, and HEK293T cells, and rat embryonic fibroblasts, the following antibodies were used: anti-Tom20 at 1:500 (FL-145, Santa Cruz Biotechnology, Inc.), anti-tubulin at 1:1000 (clone DM1A, Sigma-Aldrich), anti-GFP 1:500 (Aves Labs, Inc.), anti-myc at 1:500 (9E10, Santa Cruz Biotechnology, Inc.), anti-HA 1:500 (Cell Signaling). For secondary antibodies, the following were

used: Alexa-488, Cy5, or Cy3 conjugated anti-mouse and anti-rabbit antibodies at 1:500 (Molecular Probes, Invitrogen). DNA was visualized by Hoechst 33342 (Vybrant Apoptosis Assay Kit #5, Molecular Probes, Invitrogen) using the manufacturer's protocol.

In addition to the aforementioned antibodies, the following were used exclusively on immunoblots: anti-DIC 1:1000 (Millipore), anti-KHC 1:100 (clone H2, Millipore), anti-p150 1:1000 (BD Biosciences), anti-hMilton (TRAK1) at 1:1000 (Sigma-Aldrich), anti-Rhot1 (Miro) at 1:1000 (clone ARP44817, Aviva Systems Biology), anti-Cyclin B 1:1000 (Santa Cruz Biotechnology, Inc.), anti-ATP5β 1:5000 (Sigma-Aldrich), anti-CDK1 substrates 1:1000 (Cell Signaling). HRP conjugated anti-rabbit and anti-mouse secondary antibodies (Jackson, ImmunoResearch Laboratories, Inc.) were used for chemilumiescent detection using SuperSignal West Dura (Pierce Biotechnology, Thermo Scientific) by either using film or the ImageQuant LAS 4000 mini.

**Live-Cell Imaging**

HeLa cells were transfected with Mito-dsRed and GFP-tubulin prior to synchronization. Cells were incubated with HEPES containing DMEM without phenyl red. Z-stacks were spaced at 0.55 μm per slice. Videos were prepared using the composite z series without the first 1 μm in order to visualize the spindle better.

**Biochemical Assays**

For immunoprecipitation, HEK293T cells were transfected with myc-Milton and synchronized using thymidine and s-trityl-L-cysteine. myc-hMilton1 was immunoprecipitated as previously (Glater et al., 2006) with anti-myc (Novus).

For mitochondrial isolation, 3 million cells were suspended in 1 mL isolation buffer containing 200mM sucrose, 10mM Tris pH 7.4, 1mM EGTA and subsequently homogenized with a Dounce homogenizer. Lysates were centrifuged at 2000 g for 10 minutes to remove cellular debris and the supernatant was centrifuged at 10,000 g for 20 minutes to pellet mitochondria. For incubations with cytosol, the remaining cytosolic supernatant from interphase or mitotic cells was subject to an additional centrifugation at 16,000 g for 20 minutes to insure that no mitochondria were carried over. Mitochondrial fractions were incubated with the appropriate cytosol for two hours on the rotator at $4^{o}$C. Mitochondria were re-isolated at 10,000 g for 20 minutes. For treatment with calf intestinal phosphatase (CIP), 10x Buffer 2 (New England Biosciences) was added to mitochondrial isolation buffer along with Protease Inhibitor Set III (Calbiochem), 100 μM PMSF, and 35 units of CIP (New England Biosciences) per 50 μL. For the inactive CIP condition, 20 mM $Na_3VO_4$ was pre-incubated with CIP for 10 min. After 1 hour CIP incubation at 37 degrees Celsius, $Na_3VO_4$ was added for 10 min to inactivate the phosphatase. Incubation with the appropriately treated cytosol occurred for 2 hours at $4^0$ C and mitochondria were re-isolated at 10,000 g for 20 minutes. Mitochondria were immunoprobed for the indicated proteins

For CDK1 assays, isolated mitochondria were re-suspended in mitochondrial isolation buffer with 10x Protein Kinase Buffer (New England Biosciences), 5 mM

$Na_3VO_4$, 100 μM PMSF, Protease Inhibitor Set III, and 1 mM ATP with or without 1000 Units of CDK1 (New England Biosciences) or 1 μg of Aurora A (Sigma Aldrich) per 100 μL. Mitochondria were incubated at $30^0$C for 2 hours and after addition of 500 μL of fresh mitochondrial isolation buffer were reisolated at 10,000 g for 20 minutes to separate them from the disassociated motors. Mitochondria were immunoprobed for the indicated proteins.

For rapalog treatments, HeLa cells expressing the appropriate constructs were treated with 5 μM of the A/C Heterodimizer (Clontech) or ethanol, the vehicle control at the indicated times.

Supplemental Figure Legends

**Figure S1. Related to Figure 1. Mitochondrial Distribution in Mitotic Cells**

(A) COS-7 cells, rat embryonic fibroblasts (REF), and HEK293T cells were synchronized in mitosis. In each cell line, mitochondria (TOM20, magenta), occupy a region largely devoid of tubulin (green), and DNA (blue). (B) HeLa cells were transfected with Mito-dsRed and GFP-tubulin and synchronized. Images were taken every 2 minutes. Scale bars represent 5 microns.

**Figure S2. Related to Figure 2. Effects of actin depolymerization, STIM1 mutation, and microtubule depolymerization on mitochondrial distribution in mitosis.**

(A,B) The percent of the total mitochondrial area that overlapped with tubulin during mitosis and the asymmetric index were calculated for 30 cells, either control or latrunculin-treated, as in Figure 2A,B. Data are represented as mean ± SEM. (C,D) The percent of the total mitochondrial area that overlapped with tubulin and the asymmetric index were calculated for 30 mitotic cells transfected with STIM1 WT or STIM1 10A as in Figure 2C,D. (E) HeLa cells were transiently transfected with STIM1 WT or STIM 10A in conjunction with the ER marker RFP-Sec61B. Cells were synchronized in mitosis and imaged by confocal microscopy. Cells were also stained for tubulin (green) and DNA (blue). STIM10A relocalizes ER onto the spindle. (F) HeLa cells were synchronized in mitosis and were treated with either DMSO (Control) or Nocodazole for 10 minutes prior to fixation. Cells were imaged and stained for tubulin, mitochondria, and DNA. Scale bars represent 5 microns unless otherwise noted.

**Figure S3. Related to Figure 3. Distribution of tagged motor proteins expressed in interphase and mitotic cells.**

(A-D). HeLa cells transiently expressed myc-hMilton1 (Milton) and either (A) KIF5C-CFP (KHC), (B) DIC2C-RFP (DIC), (C) pEGFPC2-p150 (p150), or (D) HA-Miro1 (Miro). Cells were imaged during interphase and mitosis by confocal microscopy. During mitosis, each of the motor proteins is present on the spindle microtubules and also diffusely in the cytosol. For KHC, the redistribution is most apparent because in interphase it is recruited almost exclusively to mitochondria and moves the mitochondria to aggregates in the periphery of the cell. In mitosis, what overlap

of KHC and mitochondria is present is due to the diffuse KHC in the cytosol. Scale bars represent 5 microns. (E) HeLa cells were synchronized into interphase or mitosis (s-trityl-L-cysteine-induced arrest). Isolated mitochondria (Mito) were probed for each of the motor adaptor complex proteins. Levels of the motor protein subunits were reduced on mitotic mitochondria, but Milton and Miro remained on mitochondria. Anti-CyclinB is a control for mitotic phase, and the mitochondrial protein ATP5b demonstrates equal mitochondrial content of the fractions.

**Figure S4. Related to Figures 3 and 4. Mutation of Milton phosphorylation sites does not prevent motor shedding.**

(A) Myc-hMilton1 was immunoprecipitated from lysates of interphase or mitotic HEK293T cells and then incubated with calf intestinal phosphatase (CIP) either with the phosphatase inhibitor $NaVO_4$ (-CIP) or without the inhibitor (+CIP). Phosphatase treatment reversed the band-shift for mitotic Milton. (B) Schematic of the 28 sites on human Milton1 that were mutated to alanine to prevent phosphorylation. Sites were selected by a compilation of mass spectrometry of Milton immunoprecipitated from mitotic and interphase HEK293T cells (black) and some additional sites (red) added due to their match with the CDK1 target consensus S/T-P. (C) Mitochondria were isolated from cells expressing either myc-hMilton1 wild type (WT) or myc-hMilton1 with 28 alanine substitutions (28A) during interphase (I) or mitosis (M) and immunoprobed for the indicated proteins. The 28A mutation prevented the large shift in migration of Milton during mitosis, but did not prevent the shedding of the motor proteins. (D) Cells expressing HA-Miro1, GFP-Tubulin, and either myc-

hMilton1 WT or 28A were immunostained for the mitochondrial marker TOM20, Milton, and tubulin. The 28A mutation did not alter mitochondrial distribution during mitosis. (E-F) Schematic and immunoblot of an assay to determine the significance of Milton phosphorylation for motor shedding during mitosis. Mitotic cells expressing wild type myc-hMilton1 (WT) or a phosphoresistant mutant (28A) were incubated with mitotic cytosol that had been treated either with active CIP (+CIP) or CIP inhibited by the phosphatase inhibitor $NaVO_4$ (-CIP). Mitochondria were re-isolated and analyzed by immunoblot for the presence of dynein. Phosphatase treatment of the cytosol allowed some DIC re-attachment to mitotic mitochondria, but Milton 28A and WT were equivalent in the assay. (G) Mitochondria were isolated from cells expressing either KIF5C-CFP wild type (WT) or KIF5C-CFP with 2 alanine substitutions during interphase (I) or mitosis (M) and immunoprobed for the indicated proteins. The KIF5C-CFP mutations did not prevent the shedding of kinesin. (H) Cells expressing either KIF5C-CFP wild type or KIF5C-CFP 917/933A were immunostained for the mitochondrial marker TOM20, KIF5C-CFP, and tubulin. The KIF5C mutations did not alter mitochondrial distribution during mitosis.

**Figure S5. Related to Figure 5. Induced and constitutive attachment of motors to mitotic mitochondria induces their redistribution.**

(A) Schematic of the rapalog system used to target an FKBP domain (Tom20-mCherry-FKBP) to mitochondria and thereby recruit either a chimeric kinesin motor (HA-KIF5B-FRB) or the dynein adaptor BICD (HA-BICD2-FRB) to

mitochondria upon rapalog addition. (B) Schematic of chimeric proteins of BICD and the KIF5C motor domain that were directly tethered to the outer mitochondrial membrane. (C) Representative images of cells transfected with Tom20-mCherry-FKBP and HA-BICD2-FRB or HA-KIF5B-FRB were taken by confocal microscopy. Ethanol and rapalog-treated interphase cells were stained for mitochondria (magenta), tubulin (green), and DNA (blue). Rapalog addition drives mitochondria to the (-) or (+) ends of the microtubules depending on the polarity of the recruited motor. (D) HeLa cells transiently expressing GFP-Mito or GFP-BICD2-Mito (grey) were synchronized and imaged during metaphase. Cells were immunostained and pseudocolored for the mitochondrial marker TOM20 (magenta) and tubulin (green). BICD, but not the GFP control, induced mitochondria to cluster near the spindle poles.

**Figure S6. Related to Figure 6. Mitochondrial symmetry in untreated control cells.**

(A) Schematic indicating how the asymmetric index at metaphase was calculated with the equation shown. (B,C). Asymmetric indices of mitochondria (B) and tubulin (C) were calculated for 30 metaphase HeLa cells. Data are represented as median with the interquartile range. The low degree of asymmetry is comparable to that seen in the transfected cells in in Figure 5B,C in the absence of rapalog. (D) Schematic model of the asymmetric distribution of mitochondria as a consequence of microtubule association prior to centrosome migration. (E) HeLa cells in telophase were stained for mitochondria (magenta), tubulin (green), and DNA

(blue). (F-G). Asymmetric indices of mitochondria (F) and tubulin (G) in 30 telophase cells. Data are represented as median with the interquartile range. Scale bars represent 5 microns.

**Figure S7. Related to Figure 7. Dynein recruitment to mitochondria and peroxisomes.**

(A) Representative confocal images of HeLa cells transiently transfected with GFP-Mito or GFP-BICD2-Mito. Cells were immunostained and pseudocolored for the mitochondria (magenta) and tubulin (green). (B) The average percentage of multinucleated cells from three transfections as in (A) were averaged and compared by a student's t-test. Data are represented as mean ± SEM. (C) HeLa cells were transfected with PEX-RFP-FKBP and HA-BICD2-FRB and treated with ethanol (control) or rapalog. Cells were synchronized and imaged during metaphase. BICD-induced recruitment of dynein (gray) caused peroxisomes (magenta) to localize to microtubules (green) at the spindle poles. Scale bars represent 5 microns. (D) Comparison of the spindle angles in vehicle and rapalog-treated cells expressing Tom20-mCherry-FKBP and HA-BICD2-FRB. (D) Comparison of the spindle angles in vehicle and rapalog-treated cells expressing Tom20-mCherry-FKBP and HA-KIF5B-FRB. Data are represented as median with the interquartile range.

**Movie S1. Mitochondria release from microtubules during the early stages of mitosis and remain passively in the periphery.**

HeLa cells were transfected with Mito-dsRed and GFP-tubulin prior to synchronization. Images were taken every minute using a spinning disk confocal. Scale bar represents 5 microns.

**Movie S2. Mitochondria release from microtubules and are not actively moved from their locations.**

HeLa cells were transfected with Mito-dsRed and GFP-tubulin prior to synchronization. Images were taken every minute using a spinning disk confocal.

**Movie S3. Mitochondria remain detached from microtubules until completion of cell division.**

HeLa cells were transfected with Mito-dsRed and GFP-tubulin prior to synchronization. Mitochondria remain peripheral to the spindle throughout metaphase. As the cell enters anaphase and telophase, mitochondria occupy the same space as microtubules. Images were taken every 1 minute. Scale bar represents 5 microns.

**Movie S4. Mitochondria move into the spindle space once microtubules begin to depolymerize.**

HeLa cells were transfected with Mito-dsRed and GFP-tubulin prior to synchronization. Cells were treated with 100 ng/mL nocodazole and imaged every 1 minute.

**Movie S5. Dynein recruitment forces mitochondria onto the spindle apparatus.**

HeLa cells transiently expressing Tom20-mCherry-FKBP and the dynein-binding construct HA-BICD2-FRB were synchronized and treated with the heterodimizer rapalog. Images were captured every minute.

**Movie S6. Dynein-induced asymmetry of mitochondrial distribution during metaphase persists into inheritance.**

HeLa cells transiently expressing Tom20-mCherry-FKBP and the dynein-binding construct HA-BICD2-FRB were synchronized and treated with the heterodimizer rapalog. The cell outline is drawn for convenience. Rapalog treated cells begin at a 0.64 asymmetric index and end at 0.71, where as control cells start at an asymmetric index of 0.05 and finish at 0.07 at the end of mitosis. Images were captured every minute. Scale bars represent 5 microns.

**Movie S7. Kinesin-induced asymmetry of mitochondrial distribution during metaphase persists into inheritance.**

HeLa cells transiently expressing Tom20-mCherry-FKBP and the dynein-binding construct HA-KIF5B MD-FRB were synchronized and treated with the heterodimizer

rapalog. The cell outline is drawn for convenience. Rapalog treated cells begin at a 0.15 asymmetric index and end at 0.16. where as control cells start at an asymmetric index of 0.05 and finish at 0.08 at the end of mitosis. Images were captured every minute. Scale bars represent 5 microns.

## References


Blasier KR, Humsi MK, Ha J, Ross MW, Smiley WR, Inamdar NA, Mitchell DJ, Lo KW, Pfister KK (2014) Live cell imaging reveals differential modifications to cytoplasmic dynein properties by phospho- and dephosphomimic mutations of the intermediate chain 2C S84. *J Neurosci Res* **92:** 1143-1154

Cai D, Hoppe AD, Swanson JA, Verhey KJ (2007) Kinesin-1 structural organization and conformational changes revealed by FRET stoichiometry in live cells. *The Journal of cell biology* **176:** 51-63

Hoogenraad CC, Wulf P, Schiefermeier N, Stepanova T, Galjart N, Small JV, Grosveld F, de Zeeuw CI, Akhmanova A (2003) Bicaudal D induces selective dynein-mediated microtubule minus end-directed transport. *The EMBO journal* **22:** 6004-6015

Kapitein LC, Schlager MA, van der Zwan WA, Wulf PS, Keijzer N, Hoogenraad CC (2010) Probing intracellular motor protein activity using an inducible cargo trafficking assay. *Biophys J* **99:** 2143-2152

Miyamoto T, DeRose R, Suarez A, Ueno T, Chen M, Sun TP, Wolfgang MJ, Mukherjee C, Meyers DJ, Inoue T (2012) Rapid and orthogonal logic gating with a gibberellin-induced dimerization system. *Nature chemical biology* **8:** 465-470

Moughamian AJ, Holzbaur EL (2012) Dynactin is required for transport initiation from the distal axon. *Neuron* **74:** 331-343

Pekkurnaz G, Trinidad JC, Wang X, Kong D, Schwarz TL (2014) Glucose regulates mitochondrial motility via Milton modification by O-GlcNAc transferase. *Cell* **158:** 54-68

Shibata Y, Voss C, Rist JM, Hu J, Rapoport TA, Prinz WA, Voeltz GK (2008) The reticulon and DP1/Yop1p proteins form immobile oligomers in the tubular endoplasmic reticulum. *J Biol Chem* **283:** 18892-18904

Smyth JT, Beg AM, Wu S, Putney JW, Jr., Rusan NM (2012) Phosphoregulation of STIM1 Leads to Exclusion of the Endoplasmic Reticulum from the Mitotic Spindle. *Current biology : CB* **22:** 1487-1493

A

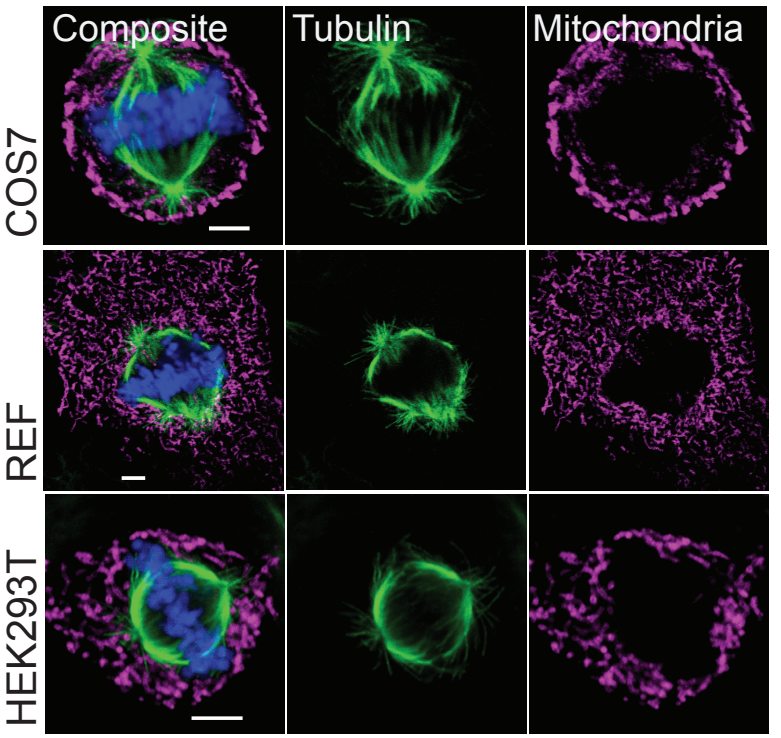
Composite
Tubulin
Mitochondria
COS7
REF
HEK293T

B

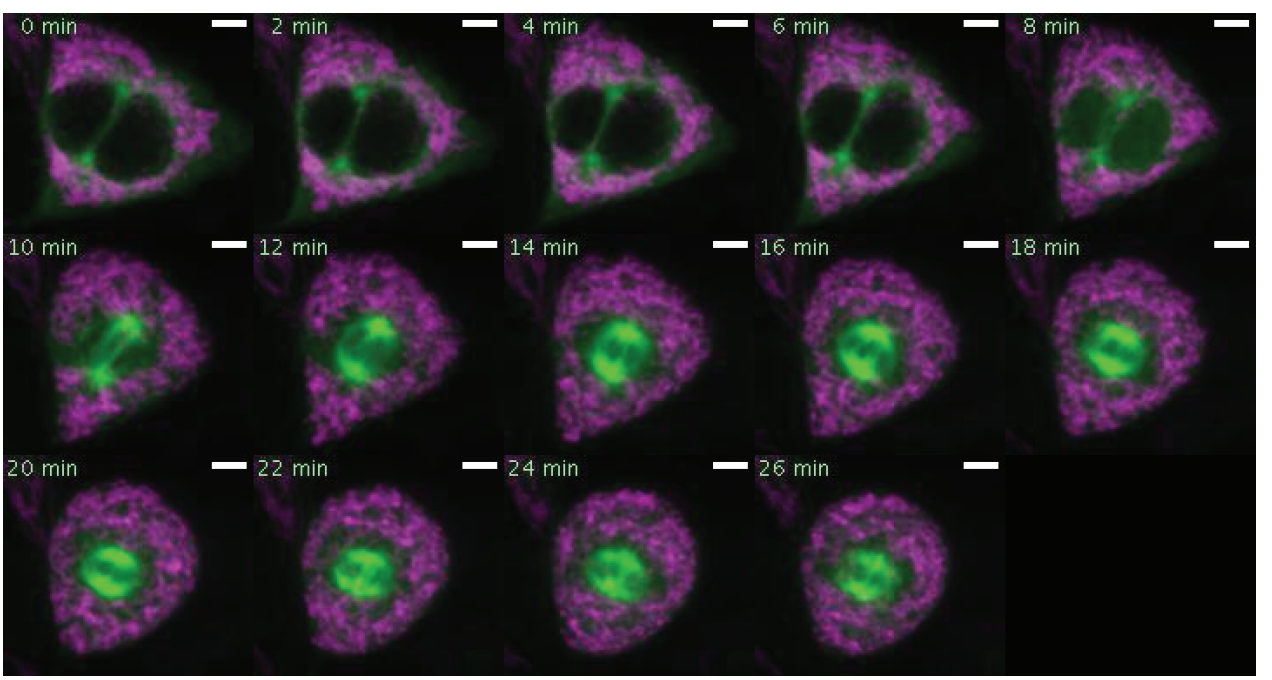
0 min
2 min
4 min
6 min
8 min
10 min
12 min
14 min
16 min
18 min
20 min
22 min
24 min
26 min

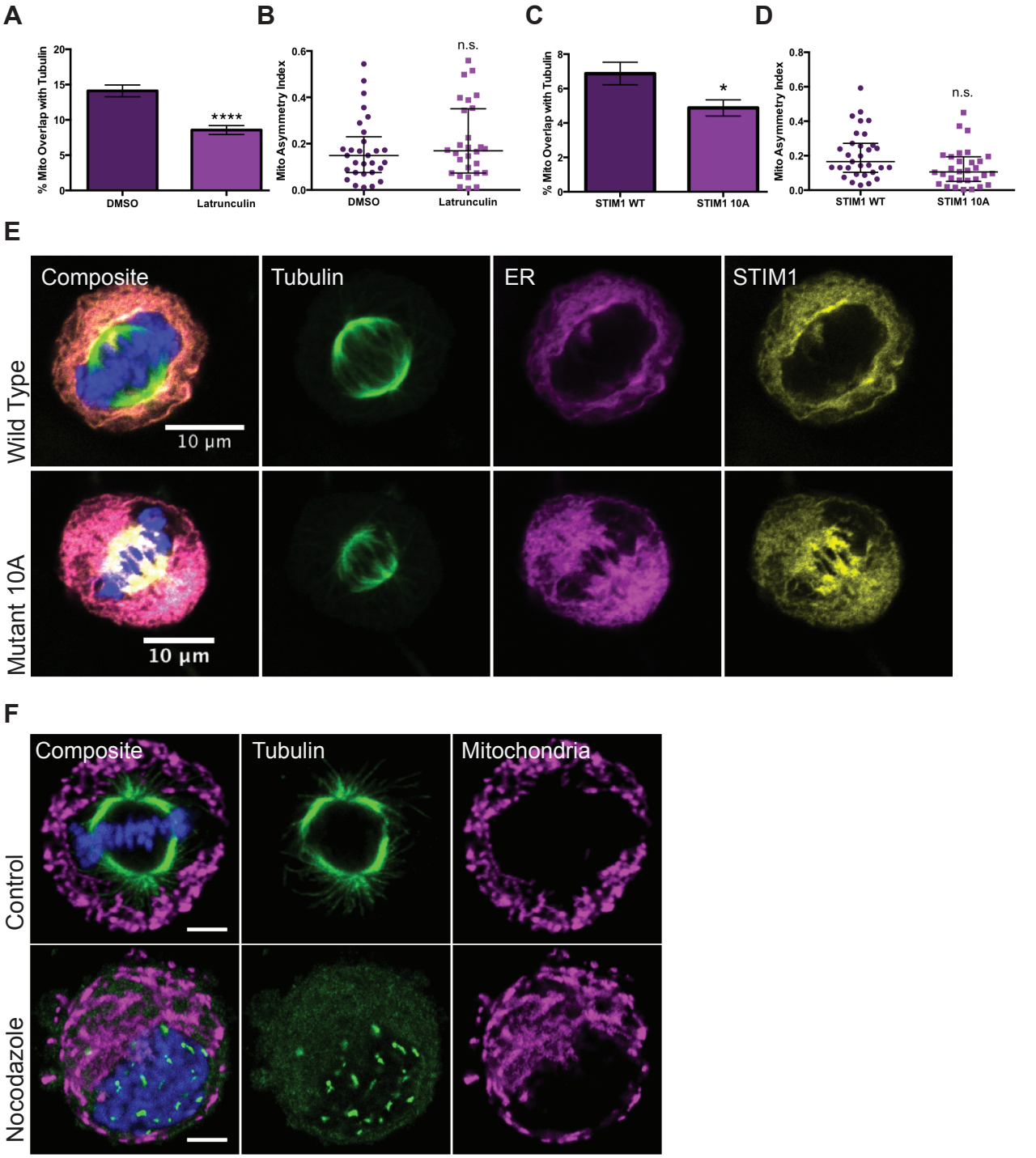
A
% Mito Overlap with Tubulin
20
15
10
5
0
****
DMSO
Latrunculin
B
Mito Asymmetry Index
0.6
0.4
0.2
0.0
n.s.
DMSO
Latrunculin
C
% Mito Overlap with Tubulin
8
6
4
2
0
*
STIM1 WT
STIM1 10A
D
Mito Asymmetry Index
0.8
0.6
0.4
0.2
0.0
n.s.
STIM1 WT
STIM1 10A
E
Composite
Tubulin
ER
STIM1
Wild Type
10 µm
Mutant 10A
10 µm
F
Composite
Tubulin
Mitochondria
Control
Nocodazole

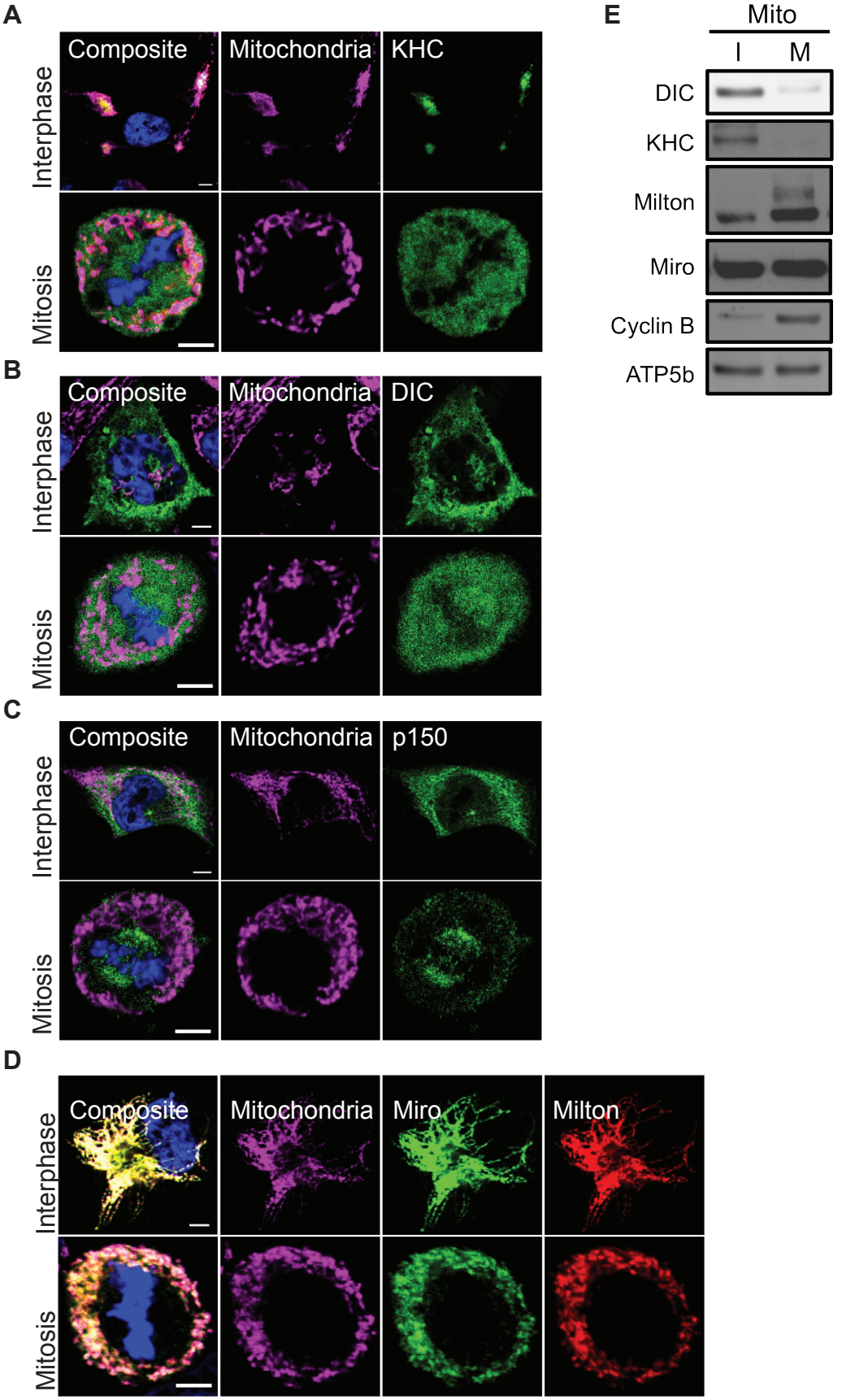
A
Composite
Mitochondria
KHC
Interphase
Mitosis
B
Composite
Mitochondria
DIC
Interphase
Mitosis
C
Composite
Mitochondria
p150
Interphase
Mitosis
D
Composite
Mitochondria
Miro
Milton
Interphase
Mitosis
E
Mito
I
M
DIC
KHC
Milton
Miro
Cyclin B
ATP5b

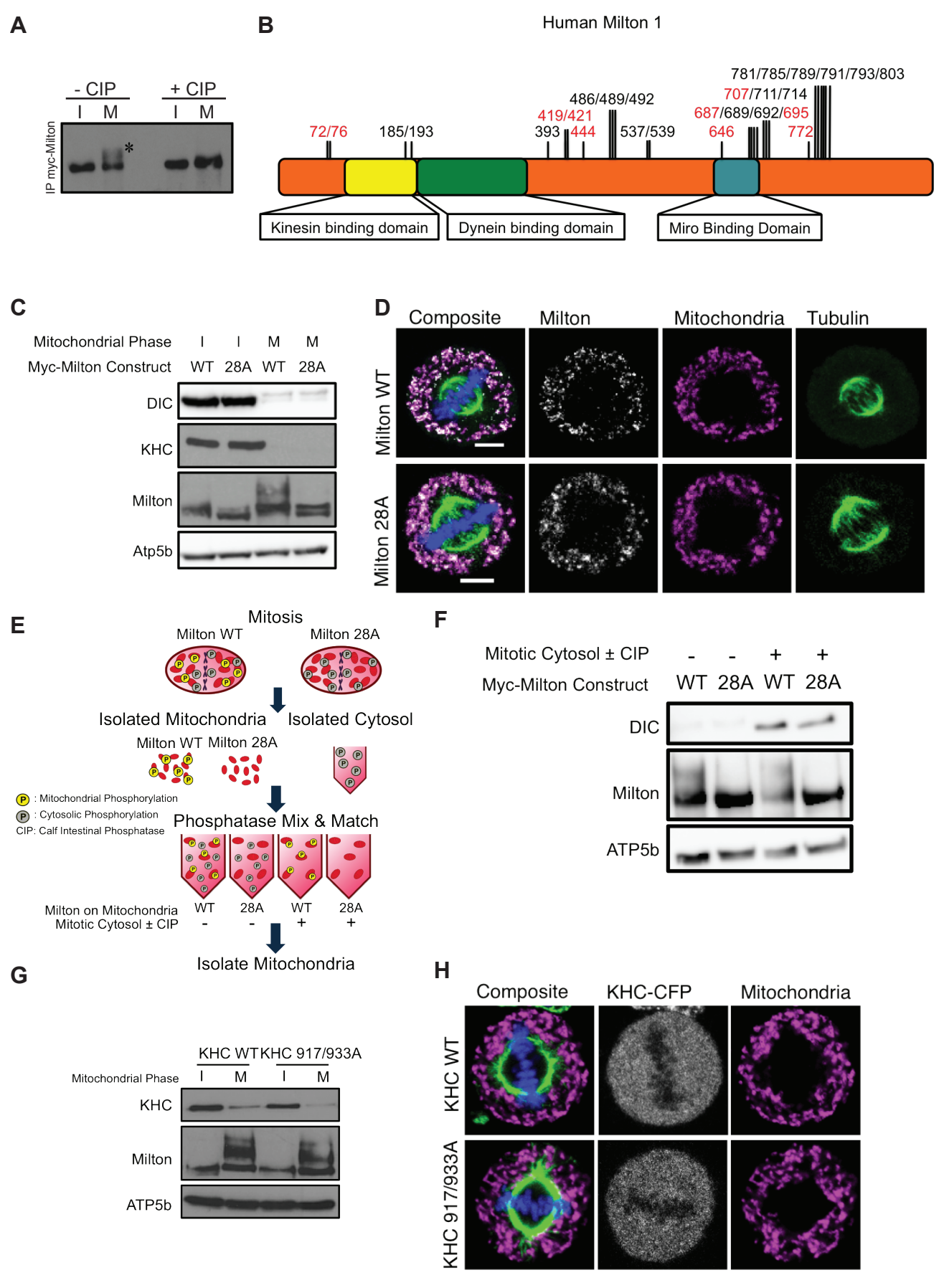
A
- CIP
+ CIP
I M
I M
IP myc-Milton
*
B
Human Milton 1
781/785/789/791/793/803
707/711/714
687/689/692/695
646
772
486/489/492
419/421
393
444
537/539
72/76
185/193
Kinesin binding domain
Dynein binding domain
Miro Binding Domain
C
Mitochondrial Phase I I M M
Myc-Milton Construct WT 28A WT 28A
DIC
KHC
Milton
Atp5b
D
Composite
Milton
Mitochondria
Tubulin
Milton WT
Milton 28A
E
Mitosis
Milton WT
Milton 28A
Isolated Mitochondria
Isolated Cytosol
Milton WT Milton 28A
: Mitochondrial Phosphorylation
: Cytosolic Phosphorylation
CIP: Calf Intestinal Phosphatase
Phosphatase Mix & Match
Milton on Mitochondria
Mitotic Cytosol ± CIP
WT 28A WT 28A
- - + +
Isolate Mitochondria
F
Mitotic Cytosol ± CIP - - + +
Myc-Milton Construct WT 28A WT 28A
DIC
Milton
ATP5b
G
KHC WT
KHC 917/933A
Mitochondrial Phase I M I M
KHC
Milton
ATP5b
H
Composite
KHC-CFP
Mitochondria
KHC WT
KHC 917/933A

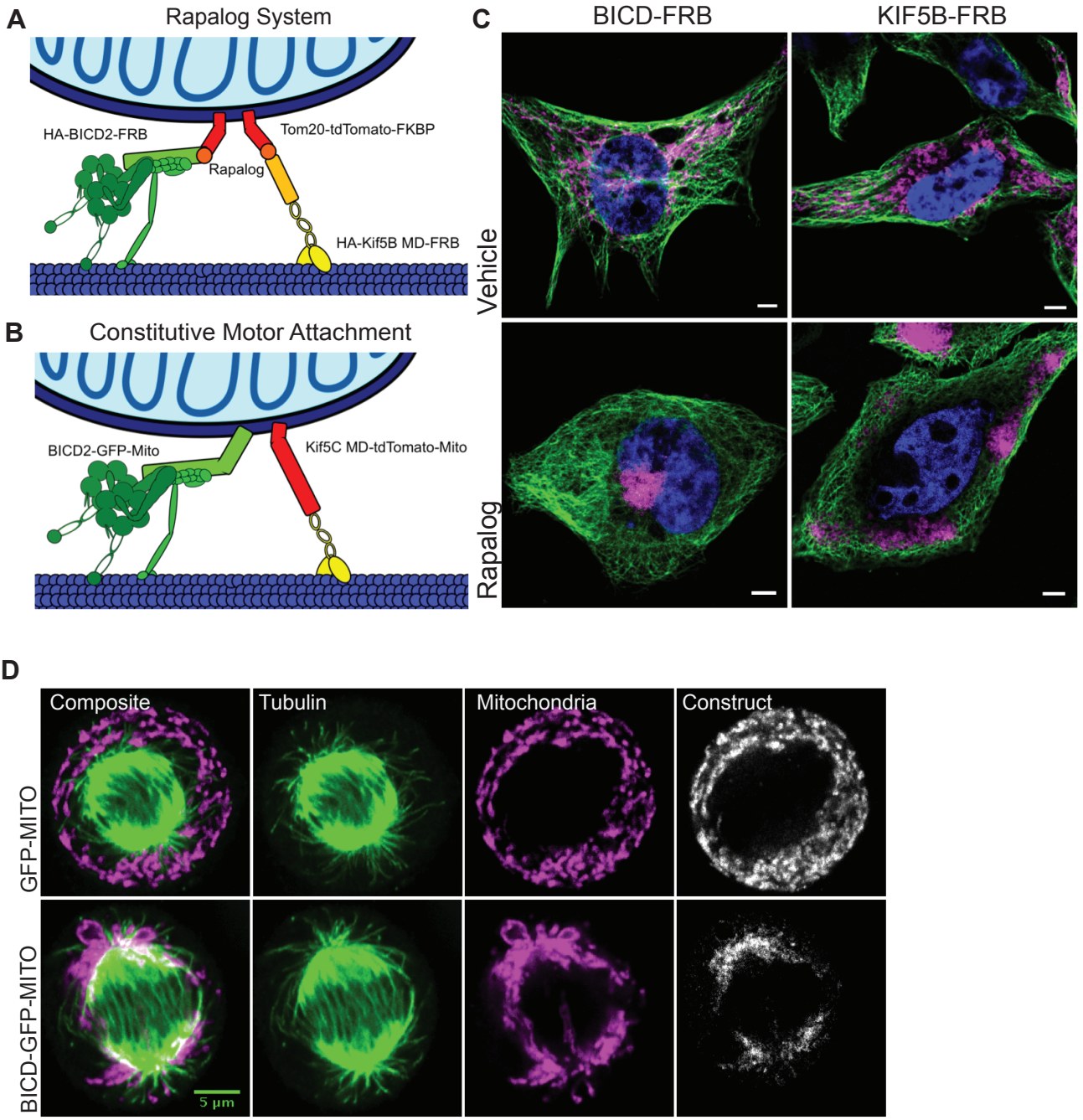
A
Rapalog System
HA-BICD2-FRB
Tom20-tdTomato-FKBP
Rapalog
HA-Kif5B MD-FRB
B
Constitutive Motor Attachment
BICD2-GFP-Mito
Kif5C MD-tdTomato-Mito
C
BICD-FRB
KIF5B-FRB
Vehicle
Rapalog
D
Composite
Tubulin
Mitochondria
Construct
GFP-MITO
BICD-GFP-MITO
5 µm

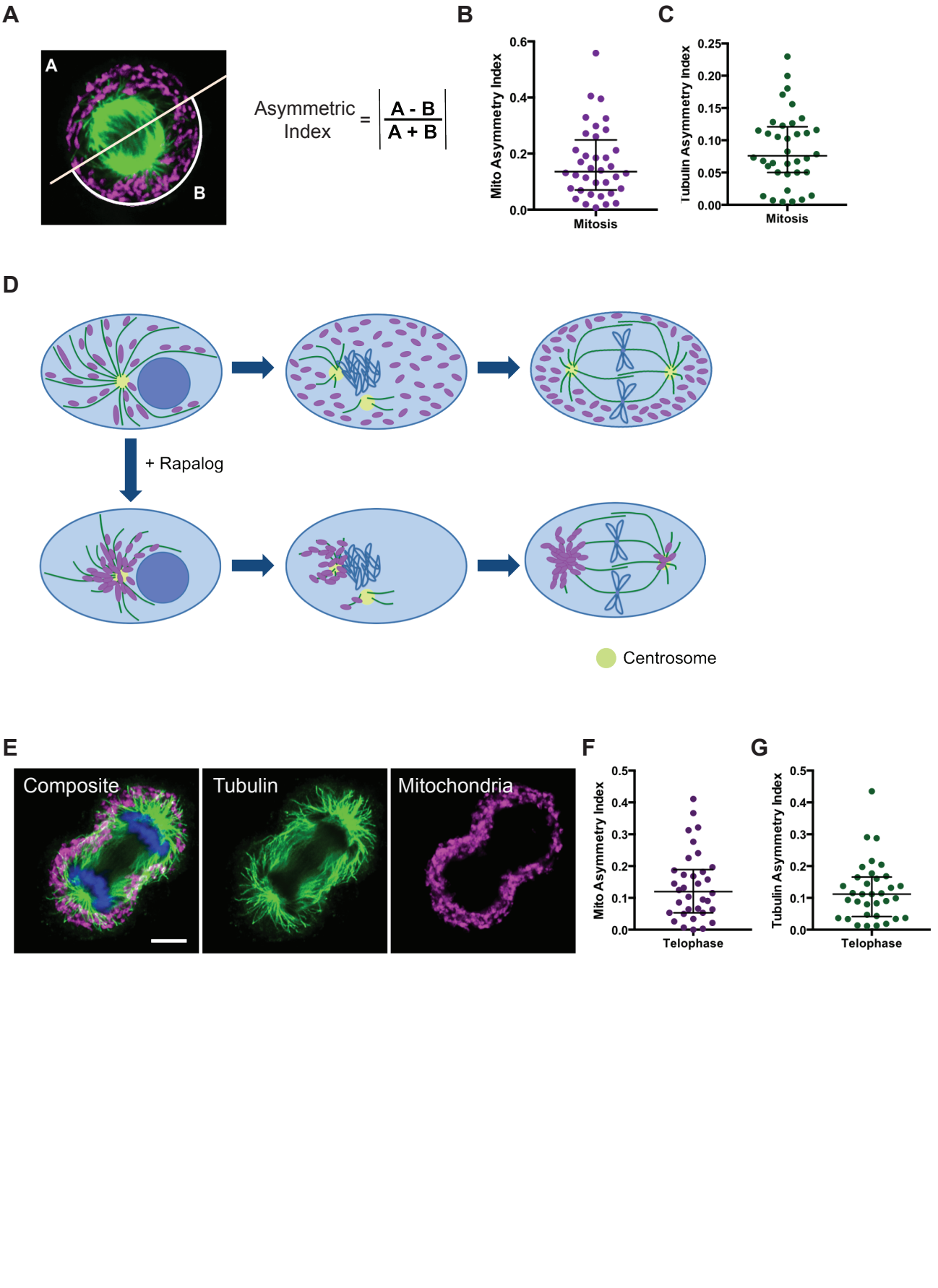
A
A
B
Asymmetric Index = |A - B / A + B|
B
Mito Asymmetry Index
0.6
0.4
0.2
0.0
Mitosis
C
Tubulin Asymmetry Index
0.25
0.20
0.15
0.10
0.05
0.00
Mitosis
D
+ Rapalog
Centrosome
E
Composite
Tubulin
Mitochondria
F
Mito Asymmetry Index
0.5
0.4
0.3
0.2
0.1
0.0
Telophase
G
Tubulin Asymmetry Index
0.5
0.4
0.3
0.2
0.1
0.0
Telophase

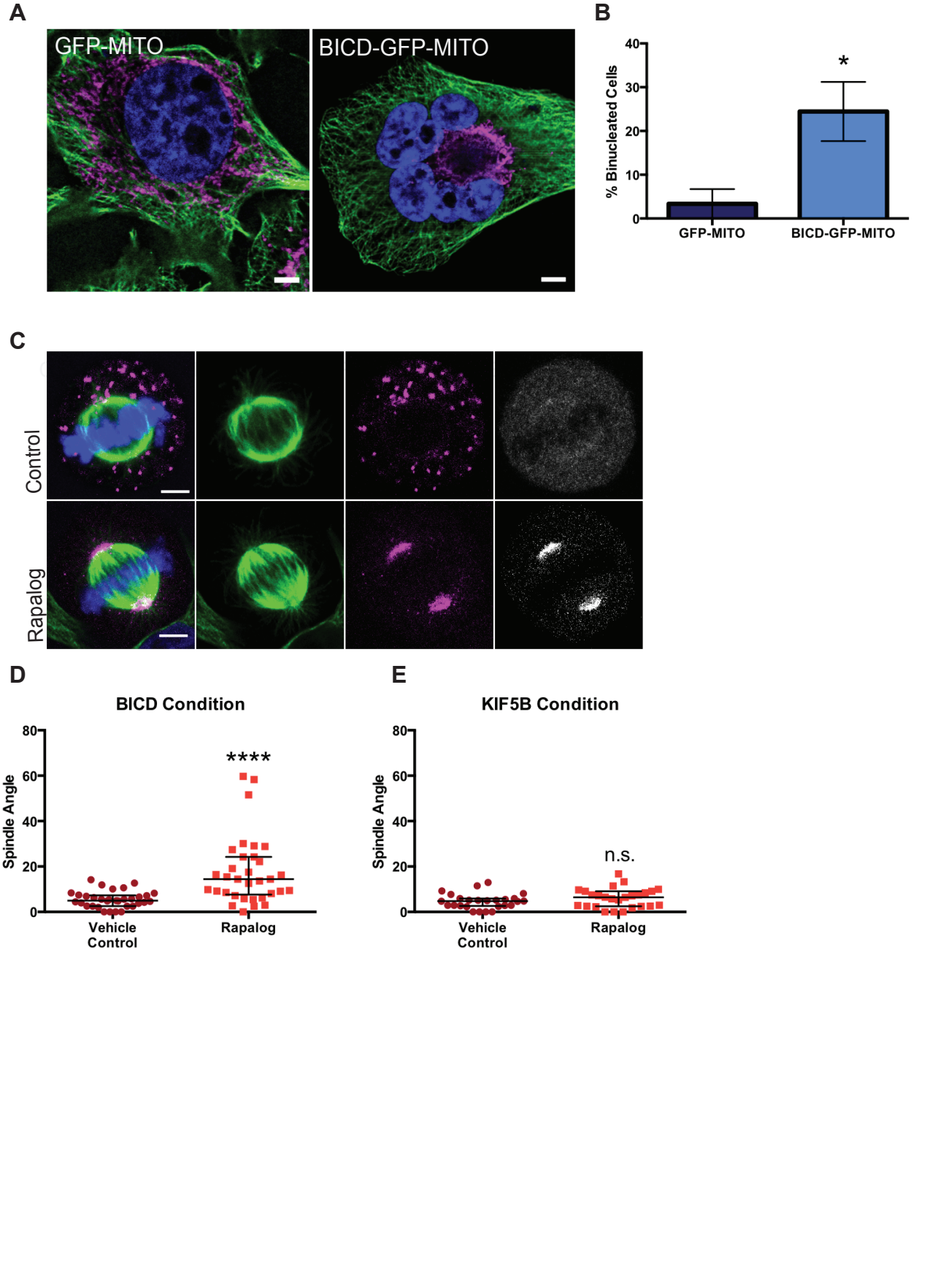
A
GFP-MITO
BICD-GFP-MITO
B
% Binucleated Cells
40
30
20
10
0
*
GFP-MITO
BICD-GFP-MITO
C
Control
Rapalog
D
BICD Condition
Spindle Angle
80
60
40
20
0
****
Vehicle Control
Rapalog
E
KIF5B Condition
Spindle Angle
80
60
40
20
0
n.s.
Vehicle Control
Rapalog